Journal of the Korean Nuclear Society
Volume 26, Number 4, December 1994

Determination of Si(Li) Detector Efficiency Using Electro-Deposition Sources in 5-15 keV Photon Energy Range

Woo Ju Jeon, Tae Soon Park, and Sun Tae Hwang
Korea Research Institute of Standards and Science
Koan Sik Joo
Myong Ji University
(Received July 18, 1994)

5-15 keV 에너지 범위에서 전기증착 선원을 사용한 Si(Li) 검출기 효율결정

전우주 · 박태순 · 황선태
한국표준과학연구원
주관식
명지대학교
(1994. 7. 18 접수)

Abstract

The full-energy peak efficiency for a collimated geometry of a Si(Li) detector has been experimentally determined using the electro-deposition sources. The radioactive sources of ^{51}Cr, ^{54}Mn, ^{57}Co and ^{65}Zn nuclides are prepared by the electro-deposition method. The measured efficiency values are corrected for the escape losses due to the K X-rays of silicon and the absorptions in materials related to source-to-detector geometry. The corrected efficiency values have turned out to be nearly constant regardless of photon energy.

요 약

Si(Li) 검출기의 full-energy peak 효율을 전기증착 선원을 사용하여 실험적으로 결정하였다. 효율결정에 사용된 측정선원은 ^{51}Cr, ^{54}Mn, ^{57}Co, ^{65}Zn 핵종으로서 전기증착 방법으로 제작하였으며, 검출기에 collimate를 설치하여 측정하였다. 산출된 효율값은 K X-선에의한 실리콘 결정에서의 탈출확률 및 측정선원과 검출기 사이의 관련 매질에 대한 감쇠효과에 대하여 보정하였으며, 보정된 효율값은 광자 에너지에 무관하게 일정하였다. 결과적으로 5-15 keV 에너지 영역에서 검출효율의 측정 정확도를 향상 시킬 수 있었다.

1. Introduction

Si(Li) and high purity germanium detectors are widely used for X- and gamma-ray measurements at low energies. The efficiency calibration of the detector is necessary for determination of the emission

rate of a radioactive source.

If the Compton scattering cross section of the detector material is negligible compared to the photoelectric cross section, the full-energy peak efficiency for a definite source-to-detector geometry can be calculated.[1] But there are several restrictions in calculating the efficiency. First, the detector thickness must be sufficient to absorb nearly all penetrating photons. Second, the effective solid angle subtended by the detector and the thickness of absorbing layer in the source-to-detector distance must be known. Third, the escape and charge collection losses from the full-energy peak must be also considered. Due to these restrictions, the detection efficiency cannot be calculated with sufficient accuracy. Therefore, efficiency curve has to be determined by means of standard source measurements.

In this work, we use standard sources which are specially fabricated for the efficiency calibration of photon detectors at low energies. The sources of ^{51}Cr, ^{54}Mn, ^{57}Co and ^{65}Zn were fabricated by electro-deposition method in order to exclude the self-absorption by the source. The efficiency of a Si(Li) detector was determined experimentally using the electro-deposited radioactive standard sources emitting X-, and gamma-rays in the energy range of 5 keV to 15 keV. The measured efficiency values were corrected for attenuation effects of radiations in air, detector-related layer, and for escape losses in the Si crystal.

2. Experiment

2.1. Source Preparation

There are several methods to prepare the thin sources of the nuclides which emit low energy photons, and the sources can be divided into quantitative and non-quantitative sources.[2, 3, 4]

Quantitative sources with known activity or photon emission rate can be obtained by depositing an aliquot of a radioactivity standard solution on supporting materials such as a metal or thin foil. But it usually consists of salt crystals giving rise to self-absorption losses which may be hard to estimate.

Non-quantitative sources for low energy photons have usually negligible self-absorption losses, but the activities or emission rates of these sources have to be determined by separate measurements. The sources can be prepared by the method of electro-deposition, vacuum evaporation or electro spraying.[5]

In this study, the efficiency of the Si(Li) detector was calibrated using ^{51}Cr, ^{54}Mn, ^{57}Co, and ^{65}Zn sources which were prepared by the electro-deposition method in the energy range from 5 keV to 15 keV. The electro-deposition sources can eliminate the self-absorption losses which are not negligible at the low energy region. The source preparation is relatively simple compared to other non-quantitative methods. In addition, deposits of good homogeneity are given by the electro-deposition.

The electro-deposition system consists of a D.C. power supply, an ampere-meter, and an electro-deposition cell as shown in Fig. 1. Separate electro-deposition cell was prepared for each nuclide to avoid the contamination by other radioactive materials. The source holder which confines a metal backing materials is used as the cathode. The platinum wire of 1mm in diameter is used as the anode and placed at the center of glass tube of 3mm in inner diameter. In order to avoid the emission of fluorescence X-rays by interaction with a backing material, stainless steel plates for ^{51}Cr, ^{54}Mn and silver plates for ^{57}Co, ^{65}Zn nuclides were used as the backing material.

The preparation method of electro-deposition source is described as the followings: One or several drops of the radioactive solution a teflon hole of 3mm in diameter and 5mm in depth. The quantity of the radioactive solution is variable according to the specific activity of the solution. The solution in the teflon hole is evaporated by using infrared lamp. Then one or two drops of HCl or NH_3 solutions are added to the mostly dried solution. The concentrated solution is transferred onto the center of polished

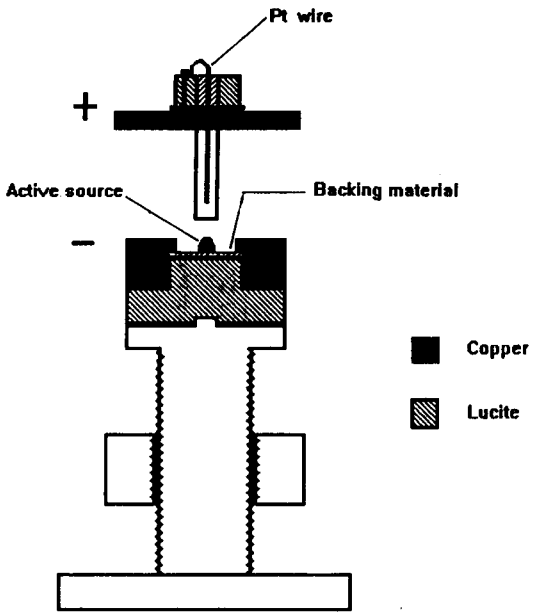

Fig. 1. Schematic Diagram of Electro-Deposition System.

backing material. The distance between anode wire and backing material is maintained by 1 to 2mm in order that the radioactive solution is electrically contacted with Pt wire by capillary action and homogeneously deposited on the backing material. The current to the electro-deposition cell was applied to be 0.2 to 2.2mA and deposition time was given to be 45 to 120min. After the electro-deposition, in order to make the uniform source, we extract the solution from backing plate by using pycnometer and clean the electro-deposited surface with distilled water. The typical deposition yield of the fabricated electro-deposition sources is shown in Table 1.

Table 1. Characteristics of Electro-Deposition for ^{51}Cr, ^{54}Mn, ^{57}Co, and ^{65}Zn Nuclides.

Nuclide	Chemical Form	Additional solution	Yield
^{51}Cr	$CrCl_2$ in 0.5 N HCl	1 N HCl	45%
^{54}Mn	$MnCl_2$ in 0.5 N HCl	0.01 N HCl	10%
^{57}Co	$CoCl_2$ in 0.5 N HCl	1 N NH_3	15%
^{65}Zn	$ZnCl_2$ in 0.5 N HCl	1 N NH_3	40%

The yield was obtained less than 50% and the amount of electro-deposition appeared to be affected by the applied current and acidic concentration of the carrier solution.

2.2. Measurement System

The X-ray spectrometry system used in this experiment consists of a Si(Li) detector with a preamplifier, an amplifier, a multichannel buffer (MCB), a personal computer, a printer, and a X-Y plotter as shown in Fig. 2.

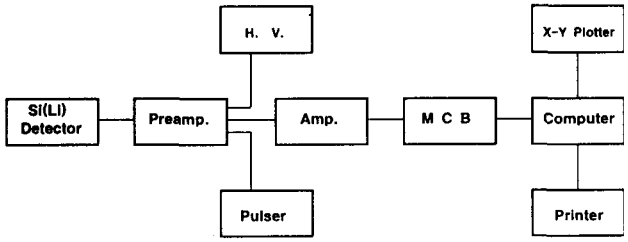

Fig. 2. Block-Diagram of X-ray Spectrometry System.

The dimension of vertical type Si(Li) detector is 16mm in active diameter and 5.48mm in sensitive depth, and its energy resolution was found to be 220 eV at 5.89 keV K X-ray energy emitted from ^{55}Fe nuclide.

A platinum collimator of 2mm in thickness and 10mm in diameter hole was placed on the surface of the detector. The collimator can confine the effective crystal volume and minimize the charge collection losses in Si crystal edge. Also, the collimator reduces the number of scattered photons from the source mount and other materials.[6] Fig. 3 shows a schematic diagram of source supporter and collimator arrangement. Platinum as a collimator material was used to avoid the fluorescence X-rays which may be emitted from interaction with photons.

The source mount was fixed at the distance of 50mm from the detector surface.

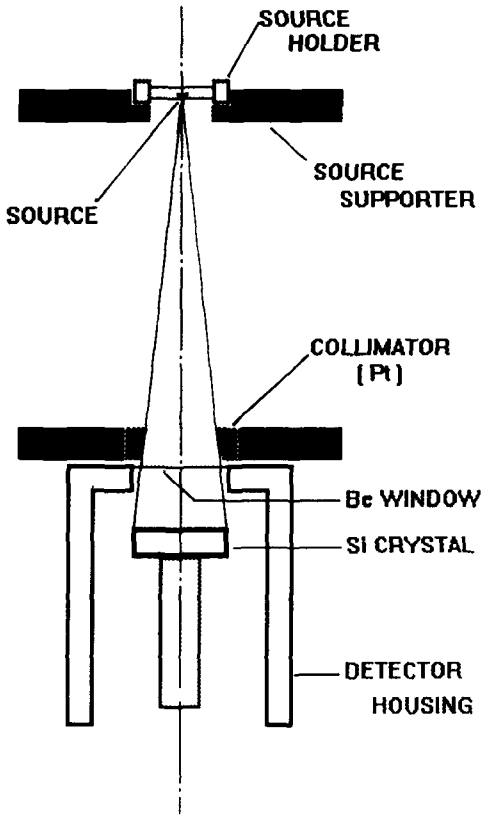

Fig. 3. Schematic Diagram of Source Supporter and Collimator Arrangement Between Source and Detector.

2.3. Measurement Procedure

The specific activity of the radioactive solution was accurately measured by the 4π(e,X)-r coincidence method. The results are given in Table 2 at the 68% confidence level.

Using these radioactive solution, thin foil sources as the quantitative source and also electro-deposition sources as the non-quantitative source were prepared, respectively. Gamma-ray spectra from these prepared sources were measured using high purity Ge detector for the energy of 122 keV and 136 keV ^{57}Co, 320 keV ^{51}Cr, 835 keV ^{54}Mn, and 1116 keV ^{65}Zn. The gamma-ray spectra were taken six times for each thin foil source being measured in both sides of the obverse and the reverse, allowing for possible asymmetric effects. Also, the gamma-ray spectra for each electro-deposition source were taken three times for the obverse side. Activity of the electro-deposition source that is non-quantitative source was obtained from the relative gamma-ray measurements using quantitative thin foil source.

Table 2. Measured Specific Activities of ^{51}Cr, ^{54}Mn, ^{57}Co, and ^{65}Zn nuclides.

Nuclide	Activity (kBq/g)	Uncertainty (kBq)
^{51}Cr	165.82	0.51
^{54}Mn	6062.04	17.58
^{57}Co	8485.06	22.91
^{65}Zn	4662.66	14.45

The X-ray and low energy gamma-ray spectra of the electro-deposition sources were measured using Si(Li) detector. Fig. 4(a)~(d) show typical X-ray spectrum measurements on the ^{51}Cr, ^{54}Mn, ^{57}Co, and ^{65}Zn sources. These plots show the K_α and K_β X-rays and the low-energy 14.4 keV gamma-ray ^{57}Co. The K_α and K_β X-rays are partially resolved doublet as shown by these plots. Therefore, the peak area was determined by summation method for the energy of 5.0 keV ^{51}Cr, 5.48 keV ^{54}Mn, 6.48 keV ^{57}Co, and 8.14 keV ^{65}Zn and by peak fitting method for the energy of 14.41 keV gamma-ray ^{57}Co as well.

3. Results and Analysis

The full-energy peak efficiency $\varepsilon(E)$ for the photon energies E was obtained from the equation

$$\varepsilon(E) = \frac{n(E)}{A \cdot P_x}, \quad (1)$$

where n(E) is count rate for the full-energy peak area of X-ray spectrum, A is activity of the source, and P_x is photon emission probability.

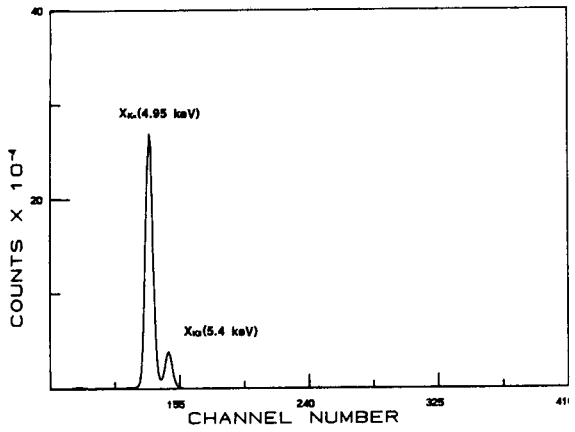

Fig. 4. (a) Pulse-height Spectrum for ^{51}Cr Observed in the Si(Li) Detector.

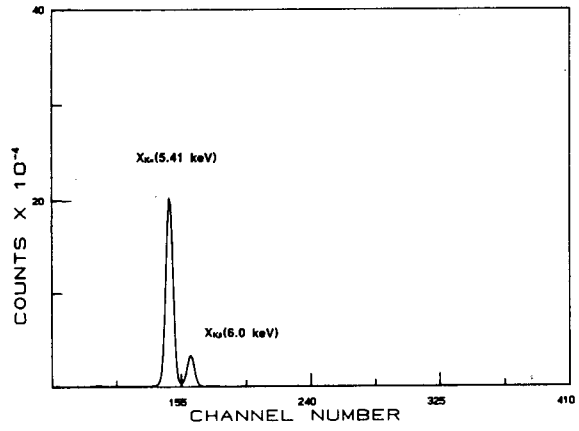

Fig. 4. (b) Pulse-height Spectrum for ^{54}Mn Observed in the Si(Li) Detector.

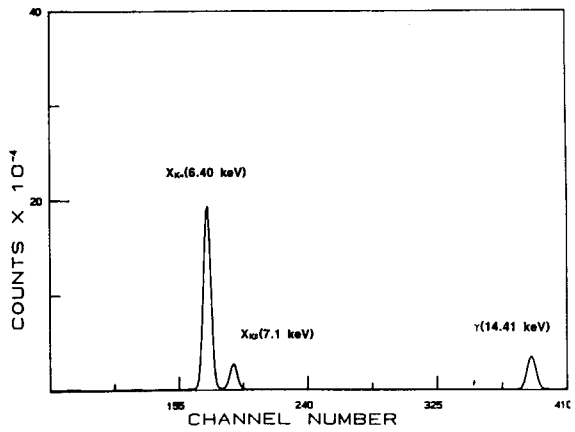

Fig. 4. (c) Pulse-height Spectrum for ^{57}Co Observed in the Si(Li) Detector.

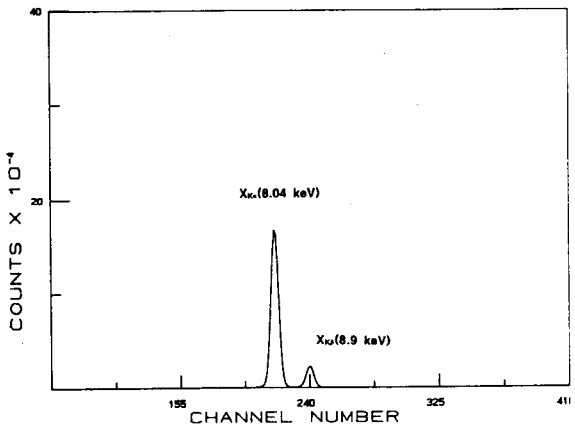

Fig. 4. (d) Pulse-height Spectrum for ^{65}Zn Observed in the Si(Li) Detector.

The full-energy peak area was corrected for dead time, decay time, and background count rates, respectively.[7] The efficiency values of Si(Li) detector are listed in column 3 of table 3 and plotted in Fig. 5. The uncertainty values listed in column 5 of table 3 were obtained from the square root of summed squares of each component uncertainty given in equation (1). The component uncertainties were taken from a standard deviation for a 68% confidence level.

The efficiency values are corrected for absorptions by air between source and detector, by detector related materials such as beryllium window, gold contact layer and silicon dead layer, and also for escape losses due to the silicon K X-rays.[8, 9]

1) In the air medium, the penetration probability of incident radiation, TR, is determined by the physical parameters according to the equation

$$TR = \exp[-\frac{\mu}{\rho} \cdot \rho_L \cdot D] \quad (2)$$

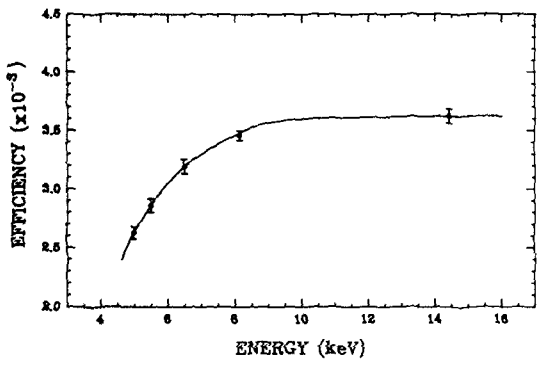

Fig. 5. Full-energy Peak Efficiency Values for Si(Li) Detector.

where μ/ρ is mass attenuation coefficient, ρ_L is air density that is corrected for temperature, humidity and atmospheric pressure, and D is distance from detector to source.

2) A beam of photons is attenuated to an intensity I from an incident intensity I_0 passing through related materials of Si(Li) detector according to the exponential absorption law

$$\frac{I}{I_0} = \exp(-\frac{\mu}{\rho} \cdot X), \quad (3)$$

where N_e is thickness of each materials given in g/cm^2. For the Si(Li) detector used in this experiment, thickness of Be window, Au electric contact layer, and Si dead layer are given 9.25×10^{-3} g/cm^2, 3.858×10^{-5} g/cm^2, and 2.33×10^{-5} g/cm^2, respectively by the manufacture's specification.

3) A beam of photons incident upon the Si detector is vertical and the escape to the sides or rear of the detector is negligible owing to the collimator. Therefore, the escape probability of incident photons can be theoretically expressed as follows[10]:

$$\frac{N_e}{N} = 0.5 \cdot \omega_k \cdot (1-\frac{1}{r})[-\frac{\mu(E_k)}{\mu(E)} \ln(1+\frac{\mu(E)}{\mu(E_k)})], \quad (4)$$

where Ne is number of counts of the escape peak, N is number of counts of the full-energy peak, ω_k is K-shell fluorescence yield of the Si(0.05), r is ratio of attenuation factors between above and below of K-edge of the Si(12.1), E_k is average energy of K X-rays of the Si(1.74keV), E is energy of incident photons, and $\mu(E)$ and $\mu(E_k)$ are attenuation coefficients of the energy E and E_k, respectively. The mass attenuation coefficients used in this work were calculated from data given by Hubbell.[11]

The corrected efficiency values and correction factors for the attenuation in the Be window, Au contact layer, and Si dead layer, and for the escape probability of the Si crystal are given in table 3, and the corrected efficiency curve are plotted in Fig. 6.

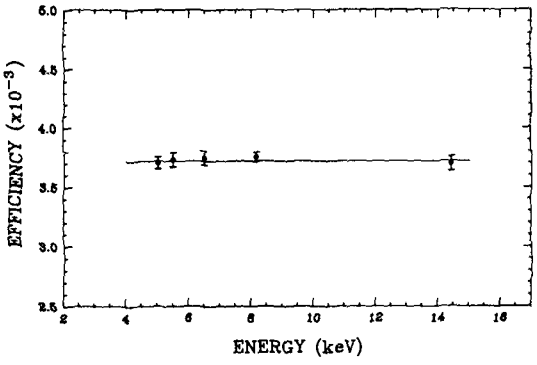

Fig. 6. Full-energy Peak Efficiency Values Corrected for Absorption and Escape.

Self-absorption of the electro-deposition source was negligible as the corrected efficiency plot results in a straight line as shown in Fig. 6. Also, it means that interaction of photons with detector crystal is mainly due to photoelectric effect in 5~15 keV energy range. The radiation attenuation effect for Si(Li) detector-related layer was decreased from 6.6% for 5.00 keV K X-ray ^{51}Cr to 1.0% 14.41 keV γ-ray ^{57}Co. The radiation attenuations in the air medium appeared to be 36% for 5.00 keV ^{51}Cr, 29% for 5.48 keV ^{54}Mn, 26% for 6.48 keV ^{57}Co, 21% for 8.14 keV ^{65}Zn, and 18% for 14.41 keV ^{57}Co. The K X-ray escape probability for Si crystal was less than 0.5%.

Table 3. Efficiency Values of Si(Li) Detector and Related Correction Factors.

Nuclide	Energy (keV)	Uncorrected Efficiency ($X 10^{-3}$)	Corrected Efficiency ($X 10^{-3}$)	Uncertainty ($X 10^{-4}$)	Correction Factors			
					Be	Au	Si	Escape
^{51}Cr	5.00 (X_k)	2.6274	3.7068	0.515	0.9640	0.9746	0.9944	0.9949
^{54}Mn	5.48 (X_k)	2.8590	3.7332	0.605	0.9690	0.9791	0.9955	0.9948
^{57}Co	6.48 (X_k)	3.1954	3.7495	0.611	0.9829	0.9865	0.9973	0.9971
^{65}Zn	8.14 (X_k)	3.4574	3.7551	0.413	0.9904	0.9923	0.9986	0.9984
^{57}Co	14.41 (γ)	3.6235	3.6994	0.621	0.9969	0.9939	0.9997	0.9998

4. Conclusions

The electro-deposition cell was designed and fabricated. The standard sources of ^{51}Cr, ^{54}Mn, ^{57}Co, and ^{65}Zn were prepared by the electro-deposition method. These sources were used to determine the efficiency of Si(Li) detector at the corresponding photon energies. The X-ray measurements were carried out using the Si(Li) detector collimated with platinum. The full-energy peak efficiency determined from the X-ray spectrum analysis was corrected for absorption materials existing between a source and the detector, and also for escape losses from Si(Li) detector. The corrected efficiency values have turned out to be nearly constant. The values show less than 1% deviation from the mean for the energy range of 5 keV to 15 keV. From these results, the emission rate of X-ray emitting nuclides can be expected to be measured with less than 1.5% uncertainty considering the measurement uncertainties of the detection efficiency and peak area. Also the pulse-height energy spectrum of X-rays was found to be produced mostly by photo-electric absorption in the energy region less than 15 keV.

References

1. K. Debertin and R.G. Helmer, *Gamma- and X-ray Spectrometry with Semiconductor Detector*, North-Holland, Amsterdam, pp. 205-189 (1988).
2. W. Van der Eijk, W. Oldenhof and W. Zehner, Nucl. Instr. and Meth., **112,** 343 (1973).
3. Y. Le Gallic, Nucl. Instr. and Meth., **112,** 333 (1973).
4. L.J. Dobrilovic and M. Simovic, Nucl. Instr. and Meth., **112,** 359 (1973).
5. G.C. Lowenthal and H.A. Wyllie, Nucl. Instr. and Meth., **112,** 353 (1973).
6. K. Debertin, J.C. Furnari and K.F. Walz, Int. J. Appl. Isot., **36,** 977 (1985).
7. K. Debertin and U. Schoetzig, Nucl. Instr. and Meth., **158,** 471 (1979).
8. J.L. Compbell and P.L. McGhee, Nucl. Instr. and Meth., **A248,** 393 (1986).
9. W.J. Gallagher and S.J. Cipolla, Nucl. Instr. and Meth., **122,** 405 (1974).
10. S.J.B. Reed and N.G. Ware, J. Phys., **E5,** 582 (1972).
11. I.H. Hubbell, Int. J. Appl. Radiat. Isot., **33,** 1269 (1982).